The small GTPase Rab22 interacts with EEA1 and controls endosomal membrane trafficking

Maria Kauppi[1], Anne Simonsen[2], Bjørn Bremnes[2], Amandio Vieira[1], Judy Callaghan[2], Harald Stenmark[2] and Vesa M. Olkkonen[1,*]

[1]Department of Molecular Medicine, National Public Health Institute (KTL), Biomedicum, PO Box 104, FIN-00251 Helsinki, Finland
[2]Department of Biochemistry, The Norwegian Radium Hospital, Montebello, N-0310 Oslo, Norway
*Author for correspondence (e-mail: vesa.olkkonen@ktl.fi)

Accepted 4 December 2001
Journal of Cell Science 115, 899-911 (2002) © The Company of Biologists Ltd

Summary

Rab22a is a small GTPase that is expressed ubiquitously in mammalian tissues and displays the highest sequence homology to Rab5. In BHK-21 cells, overexpression of the wild-type Rab22a caused formation of abnormally large vacuole-like structures containing the early-endosomal antigen EEA1 but not Rab11, a marker of recycling endosomes or the late-endosomal/lysosomal markers LAMP-1 and lyso-*bis*-phosphatidic acid. In HeLa cells, overexpressed Rab22a was found on smaller EEA1-positive endosomes, but a portion of the protein was also found in the Golgi complex. Using the yeast two-hybrid system and a biochemical pull-down assay, the GTP-bound form of Rab22a was found to interact with the N-terminus of EEA1. In HeLa cells overexpressing Rab22a or its mutants affected in the GTPase cycle, no significant changes were observed in the uptake of Alexa-transferrin. However, the GTPase-deficient Rab22a Q64L mutant caused a redistribution of transferrin-positive endosomes to the leading edges of cells and a fragmentation of the Golgi complex. In BHK cells, the Q64L mutant caused the accumulation of a fluid phase marker, TRITC-dextran, and a lysosomal hydrolase, aspartylglucosaminidase, in abnormal vacuole-like structures that contained both early and late endosome markers. Both the wild-type Rab22a and the Q64L mutant were found to interfere with the degradation of EGF. These results suggest that Rab22a may regulate the dynamic interactions of endosomal compartments and it may be involved in the communication between the biosynthetic and early endocytic pathways.

Key words: Membrane trafficking, Endosome, Golgi apparatus, GTPase, Membrane fusion, Rab effector

Introduction

Rab proteins constitute a subfamily of small GTPases that play key roles in the control of intracellular membrane trafficking. According to the prevailing view, Rab GTPases oscillate between GTP and GDP bound forms, and in the GTP conformation they recruit a variety of downstream effector proteins onto membranes (reviewed in Olkkonen and Stenmark, 1997; Chavrier and Goud, 1999; Zerial and McBride, 2001). The Rab-effector complexes are involved in diverse functions, such as transport vesicle formation (McLauchlan et al., 1998; Tisdale, 2000), tethering of vesicles at their target membranes (Waters and Hughson, 2000; Guo et al., 2000), protein phosphorylation (Ren et al., 1996) and microtubule-dependent organelle motility (Echard et al., 1998; Nielsen et al., 1999). Furthermore, increasing evidence suggests that Rabs are capable of concentrating components of the SNARE machinery responsible for the actual bilayer fusion at sites of membrane contact (McBride et al., 1999; Simonsen et al., 1999).

A strikingly high number of Rab GTPases have been localized to endosomal membrane compartments (reviewed by Rodman and Wandinger-Ness, 2000). This most probably reflects the complex organization and multiple sorting functions of endosomes (Gruenberg and Maxfield, 1995; Mellman, 1996). Material internalized from the cell surface first enters the early endosome (EE) (also called sorting endosomes), which are responsible for the dissociation and sorting of receptors and ligands. Increasing evidence suggests that EEs also receive cargo from the trans-Golgi network (TGN) through the mannose-6-phosphate receptor (M6PR) pathway (Press et al., 1998; Juuti-Uusitalo et al., 2000). These organelles are widely distributed in the cells and typically consist of vacuole-shaped and tubular subdomains. Rab5, the most thoroughly characterized member of the Rab GTPase subfamily, plays a key role in the transport of cargo from the cell surface through clathrin-coated vesicles to the EE and in the dynamic homotypic interactions between EE compartments (Novick and Zerial, 1997). Receptors that are intended for reutilization are recycled to the cell surface directly through the tubular EE subdomains or routed through a distinctive population of tubular/vesicular compartments closely apposed to the microtubule organizing center, denoted as perinuclear recycling endosomes (Hopkins, 1983; Yamashiro et al., 1984). The recycling processes are regulated by Rab4 and Rab11, and Rab4 is suggested to act at the level of the early ‘sorting’ endosomes (van der Sluijs et al., 1992), whereas Rab11 exerts a function in trafficking of cargo through the perinuclear recycling endosomes (Ullrich et al., 1996; Ren et al., 1998). A recent study employing GFP-Rab fusion proteins and live cell imaging depicted dynamic compartmentalization of different Rab proteins within the same continuous membrane (Sönnichsen et al., 2000): internalized transferrin was shown

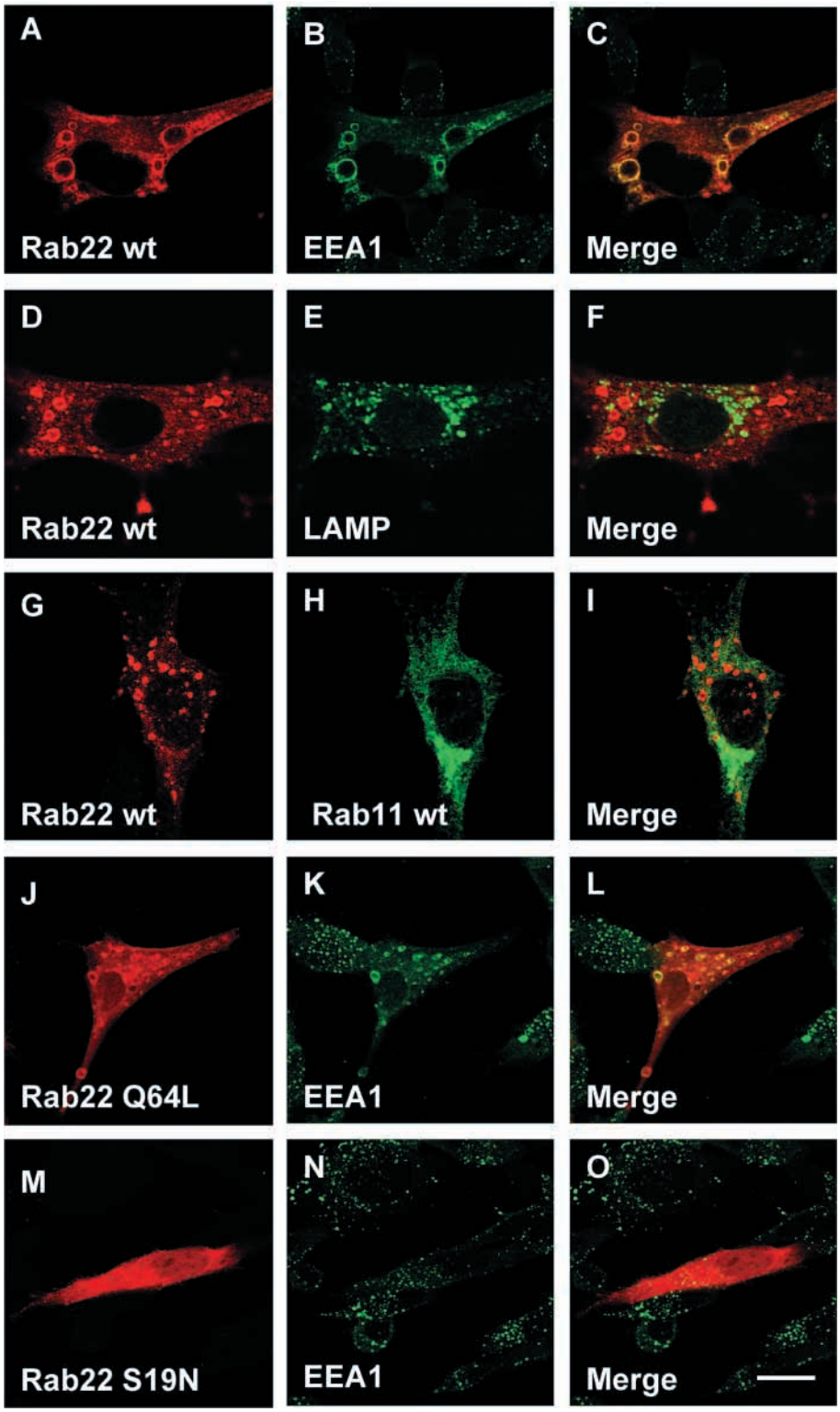

Fig. 1. Localization of Rab22a and its mutant forms in BHK-21 cells. Rab22a or the Q64L and S19N mutants were expressed by transfection of constructs in pcDNA3.1, followed by immunofluorescent double stainings to visualize the expressed protein and compartmental markers by confocal microscopy analysis. Wild-type Rab22a (A,D,G) localized on the surface of large vacuole-appearing structures, as well as on the plasma membrane. The vacuolar elements were positive for EEA1 (B) but did not contain LAMP-1 (E) or Rab11 (H). The Q64L mutant (J) showed a similar distribution and colocalized with EEA1 (K); the S19N mutant (M) displayed in many cells a diffuse cytosolic appearing staining often with additional brightly stained structures of variable size and shape in the perinuclear region. This mutant did not affect the intracellular distribution of EEA1 or show specific colocalization with it (N). Overlays are shown in panels C,F,I,L and O. Bar=10 μm.

to move from Rab5-positive to Rab5/Rab4 endosomes and then through Rab4/Rab11 containing elements to the cell surface.

Molecules destined for degradation are sorted, most probably in the vacuolar domains of EEs, to endocytic carrier vesicles that ferry them to the late endosomes (LEs) (Gruenberg and Maxfield, 1995). An alternative view is that EEs gradually mature into LEs (van Deurs et al., 1993; van Deurs et al., 1995). LEs, which are characterized by a low lumenal pH and extensive internal membranes rich in the unique phospholipid species lyso-*bis*-phosphatidic acid (LBPA) (Kobayashi et al., 1998), form another important sorting apparatus on the endocytic pathway: LEs receive lysosomally destined cargo from the EEs and the trans-Golgi-network and recycle receptors back to the TGN by a process regulated by Rab9 (Lombardi et al., 1993). Rab7 localizes to LEs and data have been presented for its function in trafficking from EEs to LEs (Feng et al., 1995; Mukhopadhyay et al., 1997; Press et al., 1998) and/or in the biogenesis of lysosomes (Meresse et al., 1995; Bucci et al., 2000).

A large number of Rab5 effector proteins have been identified (Christoforidis et al., 1999). One of these is the early endosomal antigen 1 (EEA1), a coiled-coil protein whose other hallmark property is specific interaction with phosphatidylinositol-3-phosphate (PtdIns-3-P) (Simonsen et al., 1998a; Gaullier et al., 1998). EEA1 plays a central role in the tethering of early endosomal elements (Christoforidis et al., 1999), and it has recently been shown to directly interact with SNARE proteins belonging to the syntaxin family (McBride et al., 1999; Simonsen et al., 1999). These findings have on one hand shed light on the mechanisms by which specific membrane lipids modulate vesicular transport (see Corvera et al., 1999; Huijbregts et al., 2000) and on the other provided clues to the mechanistic linkage between the Rab-based membrane tethering machinery and the SNARE-based fusion apparatus.

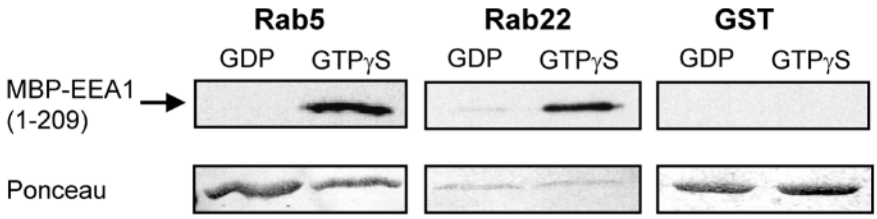

Fig. 2. *In vitro* verification of the Rab22a-EEA1 interaction. GST-Rab5a and Rab22a fusion proteins, or GST as a negative control, were bound to glutathione sepharose beads, loaded with either GDP or GTPγS and incubated with a MBP-EEA1 (aa 1-209) fusion protein as descibed in the Materials and Methods. The binding of MBP-EEA1 was visualized by SDS-PAGE and western blotting with anti-EEA1 antibodies (the top panels). Specific binding of MBP-EEA1 to the GTPγS-bound forms of both Rab5a and Rab22a was observed; the signal for the GDP-loaded proteins was very weak. Background binding of MBP-EEA1 to plain GST was undetectable. Visualization of the fusion proteins on the filters by Ponceau staining (the bottom panels) reveals that the amount of Rab22a required for a given signal intensity is markedly lower than that for Rab5a.

Rab22 is a small GTPase whose two isoforms are expressed ubiquitously at the tissue level and display the highest sequence similarity with Rab5 (Olkkonen et al., 1993; Chen et al., 1996). In the present study we report the localization of Rab22a and its mutant forms that are affected in the GTPase cycle, as well as the effects of their overexpression on endosomal and Golgi morphology and transport processes in the endocytic pathway. Furthermore, we show that, like Rab5, Rab22a interacts with EEA1.

Materials and Methods

Cell culture

Baby Hamster Kidney cells (BHK-21 clone 13) were cultured in Glasgow minimum essential medium (GMEM) supplemented with 5% foetal bovine serum (Life Technologies), 2mM L-glutamine, 10% tryptose phosphate broth, 100 U/ml penicillin and 100μg/ml streptomycin. COS-1 cells were cultured in Dulbecco's modified Eagle medium (DMEM) with 10% foetal bovine serum (FBS), supplemented with L-glutamine and antibiotics as above. HeLa and Hep2 cells were cultured in a similar medium, except that it contained 5% FBS.

Antibodies and other reagents

Rab22a was produced as an N-terminally His_6-tagged fusion protein from the pET11d expression plasmid (Invitrogen) in *Escherichia coli* BL21(DE3) (Promega), purified on Ni-NTA-agarose (Qiagen) according to a standard procedure and used for subcutaneous immunization of HsdRIVM:ELCO rabbits. A His_6-Glutathione S-transferase (GST)-tagged Rab22a fusion protein was produced using the pGAT-4 expression vector (Johan Peränen, Institute of Biotechnology, University of Helsinki). The fusion protein was purified on glutathione-Sepharose (Pharmacia), attached covalently to cyanogen-bromide-activated Sepharose 4B (Pharmacia) and used for affinity purification of Rab22a antibodies by a standard protocol. The anti-aspartylglucosaminidase (AGA) rabbit polyclonal antibody was a gift from Anu Jalanko (National Public Health Institute, Helsinki, Finland); the anti-LBPA and anti-hamster LAMP-1 monoclonal antibodies were kindly provided by Jean Gruenberg (University of Geneva, Switzerland). The anti-early endosomal antigen 1 (EEA1) rabbit polyclonal antibody was described in Simonsen et al. (Simonsen et al., 1998a); in some experiments a human autoantiserum recognizing EEA1, kindly provided by Ban-Hock Toh (Monash Medical School) was used. The anti-c-*myc* mAb was produced as ascitic fluid in Balb/c mice from the hybridoma 9E10 purchased from the European Collection of Animal Cell Cultures, and the monoclonal anti-GM130 antibody was from Transduction Laboratories. Cycloheximide and Wortmannin were purchased from Sigma and rhodamine-EGF from Molecular Probes. Human holo-transferrin (Sigma) was labelled with Alexa^{488} (Molecular Probes) according to the manufacturer's instructions.

cDNA constructs and transfection

The wild-type (wt) Rab22a cDNA (GenBank accession no: Z22820) in pGEM-myc (Olkkonen et al., 1993) was used as template for site-directed mutagenesis using the Quikchange kit (Stratagene) according to the manufacturer's instructions. The wt as well as the S19N and Q64L mutant cDNAs carrying an N-terminal myc tag were tailored by PCR to carry *Bam*HI restriction sites flanking the open reading frame at both ends. The cDNAs were inserted into the *Bam*HI site of the CMV promoter expression plasmid cDNA3.1 (Invitrogen), under the T7 promoter of pGEM1 (Promega), or in pSFV1 (Liljeström and Garoff, 1991). Transfection of BHK-21 or COS-1 cells with the

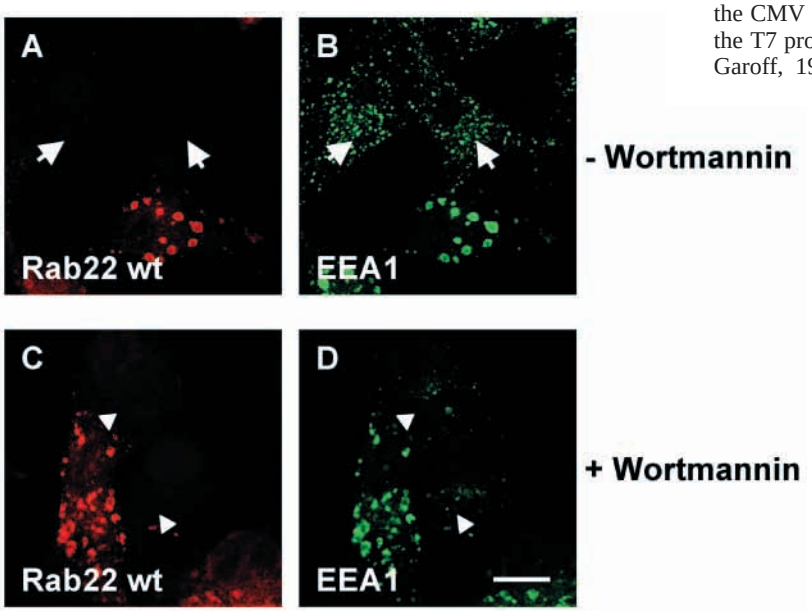

Fig. 3. Rab22a overexpression makes EEA1 resistant to Wortmannin treatment. Wild-type myc-Rab22a was expressed in BHK-21 cells for 14 hours using a recombinant SFV, the cells were then incubated for 30 minutes in the absence (–Wortmannin) or the presence (+Wortmannin) of 100 nM Wortmannin and prepared for double immunofluorescence microscopy with anti-myc and human anti-EEA1 antibodies. In untransfected cells (arrows), EEA1 showed in the absence of Wortmannin (A-B) a characteristic staining of small early endosomal structures and localized in transfected cells on the large vacuole-like Rab22a-positive endosomes. Upon Wortmannin treatment (C,D), a majority of EEA1 was lost from the endosomes of untransfected cells (arrowheads), but intense EEA1 staining remained detectable on the large Rab22a-positive endosomes of the tranfected cells. Bar=10 μm.

pcDNA3.1 constructs was carried out with the Fugene 6 reagent (Roche) according to the manufacturer's instructions using a transfection time of 24 hours. Alternatively, the proteins were expressed using recombinant Semliki Forest viruses (SFV) prepared according to Olkkonen et al. (Olkkonen et al., 1994). In some experiments, BHK-21, HeLa or Hep2 cells were infected with modified Ankara T7 polymerase recombinant Vaccinia virus (Sutter et al., 1995) for 1 hour and then transfected for 6 hours with constructs in pGEM1, before fixation and preparation for immunofluorescence microscopy. For protein expression in *E. coli* untagged wt Rab22a cDNA with flanking *Bam*HI sites created by PCR was inserted into the *Bam*HI site of pGAT-4 or pGEX1λT (Pharmacia). pET-His-Rab22a was obtained by cloning the *Nde*I-*Eco*RI and *Eco*RI-*Bgl*II fragments from pGEM-myc-Rab22a into the *Nde*I and *Bam*HI sites of pET11d (Invitrogen). cDNA encoding the 209 N-terminal amino acids of EEA1 (1-209) was cloned into pMAL-c2 (New England Biolabs), for generation of maltose binding protein (MBP)-EEA1$_{1-209}$ fusion protein (Simonsen et al., 1998a).

Immunofluorescence microscopy

The cells were fixed for 20 minutes at room temperature with 4% paraformaldehyde, 250 mM Hepes, pH 7.4 and permeabilized for 20 minutes with 0.1% Triton X-100 in PBS. The primary antibodies diluted in 5% foetal calf serum/PBS were incubated for 1 hour at 37°C and the bound antibodies were detected with fluorescein-isothiocyanate (FITC)- or tetramethylrhodamine-isothiocyanate (TRITC)-conjugated goat anti-rabbit or anti-mouse F(ab)$_2$ (Immunotech) or Cy-5-conjugated donkey anti-rabbit or anti-mouse IgG (Jackson ImmunoResearch Laboratories). In some experiments TRITC-conjugated donkey anti-mouse IgG, FITC-conjugated donkey anti-mouse IgG or FITC- or TRITC-conjugated anti-human IgG (Jackson ImmunoResearch Laboratories) were used. The specimens were mounted in Mowiol (Calbiochem), 50 μg/ml 1,4 diazabicyclo-[2.2.2]octane (Sigma) and investigated using a laser scanning confocal microscope (Leica SP1 or TCS NT). In some experiments cells were permeabilized with 0.05% saponin prior to fixation (Simonsen et al., 1998b).

Yeast two-hybrid analysis

The yeast reporter strain L40 (Vojtek et al., 1993) was cotransformed with the indicated pLexA and pGAD plasmids, and β-galactosidase activities of duplicate transformants were determined as described in Guarente (Guarente, 1983).

In vitro binding of Rab22 to EEA1

For in vitro binding of EEA1, GST-tagged Rab5a or Rab22a produced from pGEX1λT were bound to Glutathione Sepharose beads (Pharmacia) in 20 mM Hepes, 100 mM potassium acetate, 0.5 mM $MgCl_2$, 1 mM DDT, 2 mM EDTA, pH 7.2. The bound proteins were loaded with 10 μM GDP or GTPγS for 1 hour at 37°C. MBP-EEA1$_{1-209}$-fusion protein (1 μM) and 100 mM $MgCl_2$ were added on ice in the presence 10 mg/ml albumin and incubated with the beads for 1 hour at 4°C, followed by washes with 20 mM Hepes, 100 mM KAc, 5 mM $MgCl_2$, 1 mM DDT, pH 7.2. The bound proteins were eluted with 10 mM reduced glutathione for 20 minutes at room temperature and analysed by SDS-PAGE and western blotting with anti-EEA1 antibodies.

Analysis of transferrin endocytosis

HeLa cells (used one day after seeding 5×10^4 cells per coverslip) were transfected with pGEM-mycRab22a wt, -mycRab22a Q64L or -mycRab22a S19N using the Vaccinia system. Six hours after the transfection, the cells were washed three times in PBS and then incubated with Alexa^{488}-conjugated transferrin in Hepes-buffered medium containing 2 mg/ml BSA for 30 minutes at 37°C. The cells were then washed three times in PBS and permabilized with 0.05% saponin prior to fixation in 3% PFA.

Analysis of EGF uptake and degradation

Hep2 cells (used one day after seeding 3×10^4 cells per coverslip) were transfected with pGEM-mycRab22a wt, -mycRab22a Q64L, or -mycRab22a S19N using the Vaccinia system. 5 hours after the transfection the cells were incubated with rhodamine-labelled EGF (200 ng/ml) in Hepes-buffered medium containing 2 mg/ml BSA for 1 hour at 37°C. The cells were then washed three times with Hepes-buffered medium and then incubated further for 3 hours in Hepes-buffered medium containing 10 μg/ml cycloheximide. The cells were thereafter washed three times in PBS and permabilized with 0.05% saponin prior to fixation in 3% PFA.

TRITC-dextran uptake

To analyze the endocytic trafficking of TRITC-dextran, BHK-21 cells were transfected with mycRab22a wt, S19N or Q64L cDNA in pcDNA3.1 for 24 hours. The cells were incubated for 30 minutes on ice in air-medium [EAGLE MEM (Sigma), 0.292 g/l L-glutamine, 1 g/l glucose, 0.35 g/l $NaHCO_3$, 10 mM Hepes, pH 7.4], 5% foetal bovine serum, to prevent adsorption of the dextran conjugate to the cell surface. Thereafter they were labeled for 1 hour at 37°C with 5 mg/ml TRITC-dextran (10 kDa; Molecular Probes) in air-medium and fixed immediately or after 3 hours chase with complete medium and double immunostained with anti-EEA1 and anti-LAMP-1 antibodies. Double stainings were also carried out using the anti-myc mAb 9E10 for Rab22a and the above compartment marker antibodies.

Analysis of the intracellular trafficking of AGA

BHK-21 cells were double transfected with mycRab22a wt or mutant pcDNA3.1 constructs and a human AGA/pSVPoly expression plasmid (Anu Jalanko, National Public Health Institute, Helsinki, Finland) using Fugene 6 (Roche). After 24 hours, fresh culture medium containing 25 μg/ml cycloheximide was added and the incubation was continued for 3 hours. Thereafter the cells were fixed and triple stained with rabbit antibodies against AGA, human anti-EEA1 autoantiserum, and an anti-LBPA monoclonal antibody. In some triple stainings the anti-LBPA mAb was replaced with the anti-myc mAb 9E10 to visualize the myc-tagged Rab22a.

Results

Localization of Rab22a

We previously cloned Rab22a cDNA from the canine epithelial cell line MDCK II, showed that the mRNA is expressed ubiquitously in mammalian tissues and that the protein localizes to endosomal elements in BHK-21 cells (Olkkonen et al., 1993). To investigate the function of this novel GTPase, we generated mutant proteins affected in the GTPase cycle: S19N, which is equivalent to dominant inhibitory-type mutants in other Rab proteins, and Q64L, which represents an activated GTPase-deficient mutant (see Olkkonen and Stenmark, 1997). The wild-type protein and these mutants, tagged at the N-terminus with a c-*myc* epitope, were transiently expressed in baby hamster kidney (BHK-21) cells by using the CMV promoter expression vector pcDNA3.1 or the Vaccinia T7 expression system employing cDNAs under the T7 promoter of pGEM-1. Experiments were also carried out using recombinant Semliki Forest viruses (SFV) expressing Rab22a. The wild-type (wt) protein localized, as judged by immunofluorescence microscopy, to the surface of

large cytoplasmic vacuolar-appearing structures. Additionally, labeling of the plasma membrane was often detectable (Fig. 1A,D,G). The vacuolar structures coincided extensively with a marker of early endosomes, EEA1 (Fig. 1A-C), while no significant overlap was observed with the late endosomal/lysosomal markers LAMP-1 (Fig. 1D-F) and lyso-*bis*-phosphatidic acid (LBPA, not shown), nor with Rab11, a marker of the perinuclear recycling endosome compartment, which was introduced into the BHK-21 cells by cotransfection (Fig. 1G-I). The vacuole-like Rab22a-positive structures were thus identified as abnormally large early endosomes. The effect of Rab22a on endosome morphology was not specific for the BHK-21 cells, since enlarged endosomal elements were generated upon Rab22a overexpression also in other cell lines, such as COS-1, MDCK II, and Hep2, although the size of the Rab22-positive endosomes varied between the cell lines (data not shown). Furthermore, similar results were obtained with all three expression systems employed. The distribution of the Q64L mutant resembled that of the wt protein, being characterized by large cytoplasmic vacuole-like EEA1-positive structures (Fig. 1J-L). The S19N mutant showed in most of the cells a diffuse cytosolic-appearing distribution, often with additional brightly stained cytoplasmic structures of variable size and shape in the perinuclear region (Fig. 1M-O). Many of these structures did not specifically coincide with any of the compartmental markers tested and are thus likely to represent cytoplasmic protein aggregates, while some showed overlap with markers of the Golgi apparatus (data not shown). In cells expressing the S19N mutant, the EEA1-positive early endosomal compartments displayed a normal size and distribution (Fig. 1N). Interestingly, in HeLa cells, wild-type and Q64L mutant Rab22a showed prominent colocalization with markers of the Golgi complex, whereas only part of the protein localized to endosomes. At high expression levels, effects on Golgi morphology were also apparent (see paragraph Effects of Rab22a overexpression on the Golgi apparatus). From these data it is obvious that the distribution of Rab22a between the Golgi and early endosomes varies between different cell lines.

Interaction of Rab22a with EEA1

Prompted by the fact that Rab5 is the closest homologue of Rab22a (52% identical) (Olkkonen et al., 1993), we tested using the yeast two-hybrid system whether Rab22a is also capable of interacting with EEA1 (Table 1). In the β-galactosidase reporter assay, we used Rab22a cDNAs from which the C-terminal double cysteine motif was removed (marked with ΔC in Table 1) to facilitate the transport of the fusion proteins to the yeast nucleus and thus improve the signal. This motif is subject to isoprenyl modification and is required for the association of Rabs with membranes (see Olkkonen and Stenmark, 1997). Rab22a Q64LΔC displayed a strong interaction with full-length EEA1 and even stronger with the N-terminal fragment (aa 1-209), whereas no interaction was detected with a C-terminal fragment (aa 1257-1411). A similar result, albeit with lower signals, was obtained when the EEA1 N- or C-terminal fragments were used as baits and Rab22a Q64LΔC as prey (not shown). The Rab22a wt and S19NΔC proteins showed no signal above background with any of the EEA1 preys. The drastic difference between the Rab22a Q64L and S19N mutants argued for the specificity of the observed interaction and suggested that EEA1 only interacts with the GTP-bound form of Rab22a. Why Rab22 wt ΔC showed no significant interaction with EEA1 is not clear; one possible explanation is that in yeast there could be a GAP activity that stimulates GTP hydrolysis by Rab22a with high efficiency. It is noteworthy that while Rab22a only seems to interact with the N-terminal region of EEA1, Rab5a has been shown to have two binding sites, at both the N- and the C-terminus of EEA1 (Simonsen et al., 1998a).

Table 1. Interaction of Rab22a with EEA1: two-hybrid analysis

pLexA[1]	pGAD[2]	β-gal units
Rab22 wt ΔC[3]	EEA1 full-length	0.099±0.0
Rab22 wt ΔC	EEA1 N-term[4]	0.092±0.007
Rab22 wt ΔC	EEA1 C-term[5]	0.088±0.002
Rab22 Q64L ΔC	EEA1 full-length	110.53±3.99
Rab22 Q64L ΔC	EEA1 N-term	361.45±24.25
Rab22 Q64L ΔC	EEA1 C-term	0.073±0.009
Rab22 S19N ΔC	EEA1 full-length	0.034±0.009
Rab22 S19N ΔC	EEA1 N-term	0.113±0.013
Rab22 S19N ΔC	EEA1 C-term	0.145±0.002

[1]pLexA and [2]pGAD were used as bait and prey vectors, respectively. [3]ΔC indicates Rab22 cDNAs missing the 3′ codons for two C-terminal cysteines, subject to isoprenyl modification.[4]EEA1 N-term indicates a cDNA fragment encoding EEA1 amino-acid residues 1-209 and [5]EEA1 C-term a fragment encoding residues 1257-1411.

To verify the interaction of Rab22a and EEA1 biochemically, Rab5a and Rab22a were expressed as fusion proteins with glutathione-S-transferase (GST) in *E. coli* and bound on glutathione-sepharose beads. The fusion proteins were then loaded with either GDP or the non-hydrolyzable analogue GTPγS, and pull-down experiments of soluble N-terminal fragment (aa 1-209) of EEA1 fused with maltose binding protein (MBP) were carried out (Fig. 2). In this assay, the GTPγS-loaded Rab5a was capable of specifically interacting with EEA1, whereas the GDP-bound protein showed only very low affinity for the EEA1 fragment. Similarly, the GTPγS-bound Rab22a displayed specific binding to EEA1; only a weak signal was detectable with the GDP-bound form of the protein. On the basis of Ponceau red staining of the nitrocellulose filters, approximately 5-10-fold less of the GTPγS-bound Rab22a than Rab5a was required to obtain a given signal intensity in this binding assay.

To obtain more evidence for the interaction between Rab22a and EEA1 in live cells, we employed the PtdIns-3-kinase inhibitor Wortmannin, which by abolishing the generation of PtdIns-3-P detaches EEA1 from early endosomal membranes. By overexpressing Rab5a it is possible to overcome the effect of Wortmannin and lock EEA1 on the endosomal membranes (Simonsen et al., 1998a). After 30 minutes of treatment of BHK-21 cells with 100 nm Wortmannin, the characteristic early endosomal EEA1 immunofluorescence staining was very weak in mock-transfected BHK-21 cells, indicating detachment of EEA1 from the early endosomal membranes (see Simonsen et al., 1998a). However, in cells overexpressing wt Rab22a, EEA1 remained attached to the large vacuolar endosomes harbouring the overexpressed GTPase (Fig. 3), arguing that Rab22a indeed interacts with EEA1 and is capable of recruiting it onto the endosomal membranes.

Effects of Rab22a overexpression on endocytic functions

The overexpression of Rab5a or its GTPase-deficient mutant form Q79L (Hoffenberg et al., 1995) has been shown to enhance the rate of endocytosis of transferrin (Tfn) (Bucci et al., 1992; Stenmark et al., 1994), and in the case of Rab5a Q79L simultaneous inhibition of recycling to the cell surface was observed (Stenmark et al., 1994). We therefore investigated the effects of Rab22a wt and the S19N and Q64L mutants on the uptake and cellular distribution of Alexa-labeled human Tfn in HeLa cells. This cell line was chosen because of its abundant expression of Tfn receptors and resulting efficient uptake of the human Tfn conjugate. After Vaccinia T7 infection, the cells were transfected with mycRab22a/pGEM1 constructs for 6 hours. Alexa-Tfn was then bound on the cells and internalized for 30 minutes, and the labeled Tfn, as well as the expressed GTPase, were visualized by confocal microcopy (Fig. 4). In cells expressing wt Rab22a, no change in the amount or distribution of internalized Alexa-Tfn was observed as compared to untransfected cells (Fig. 4A-E). Enlarged vacuolar endosomes such as those induced in BHK cells were rarely observed in HeLa cells, which are known to have smaller and more tubular endosomes; In these cells the expressed GTPase showed a finer punctate staining pattern, which overlapped with EEA1 (not shown) and the internalized Tfn (Fig. 4C-E), as well as a prominent perinuclear localization (Fig. 4C,F,I). Also in cells overexpressing Rab22a Q64L, the size of Alexa-Tfn-positive endosomes appeared similar to that in untransfected cells. However, the distribution of the marker was significantly altered: instead of a relatively even cytoplasmic distribution, the Tfn-positive endosomal structures were in Q64L expressing cells clustered near the cell surface at the leading

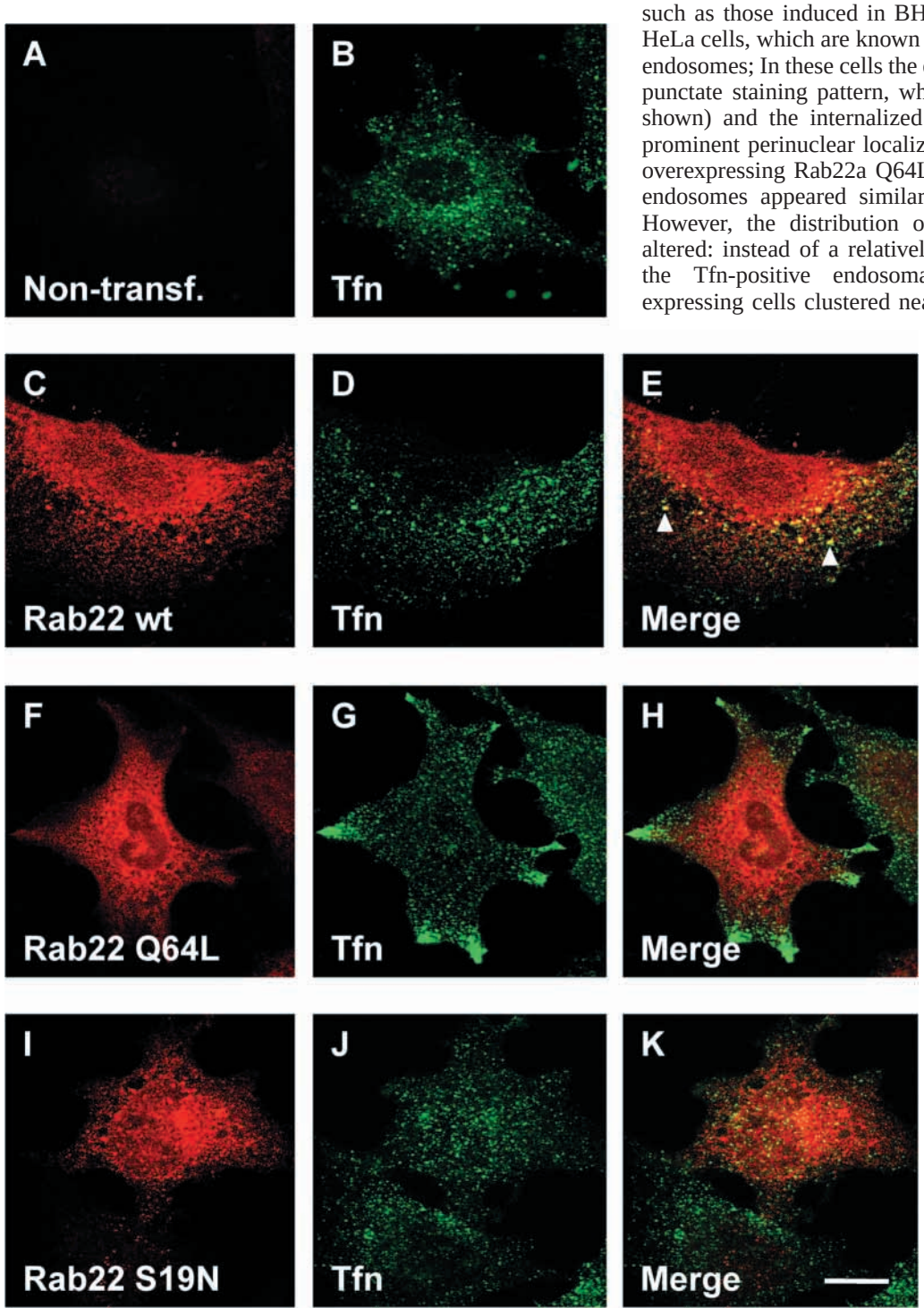

Fig. 4. Effects of Rab22a overexpression on the uptake and intracellular distibution of Alexa-transferrin (Tfn). HeLa cells were infected with the Ankara strain Vaccinia T7 virus, followed by transfection of myc-tagged Rab22a wt, Q64L or S19N constructs in pGEM-1. Cell-surface binding and uptake (30 min) of Alexa-Tfn were then carried out as described in Materials and Methods, and the cells were processed for confocal immunofluorescence microscopy. Immunostaining for Rab22a is shown in A,C,F,I; Alexa-Tfn fluorescence in panels B,D,G,J; and overlays in E,H,K. In non-transfected cells (A,B), the Tfn was observed in characteristic endosomal structures. The volume or distribution of these structures was not significantly affected by expression of wt Rab22a (C-E). However, in cells expressing Rab22a Q64L (F-H) the Alexa-Tfn containing endosomes were redistributed to clusters near the leading edge. The Rab22a S19N mutant (I-K) had no detectable effect on the volume or distribution of internalized Alexa-Tfn. The wt Rab22a (E, arrowheads), but not the mutant proteins (H,K), showed a partial colocalization with Alexa-Tfn. Bar=10 μm.

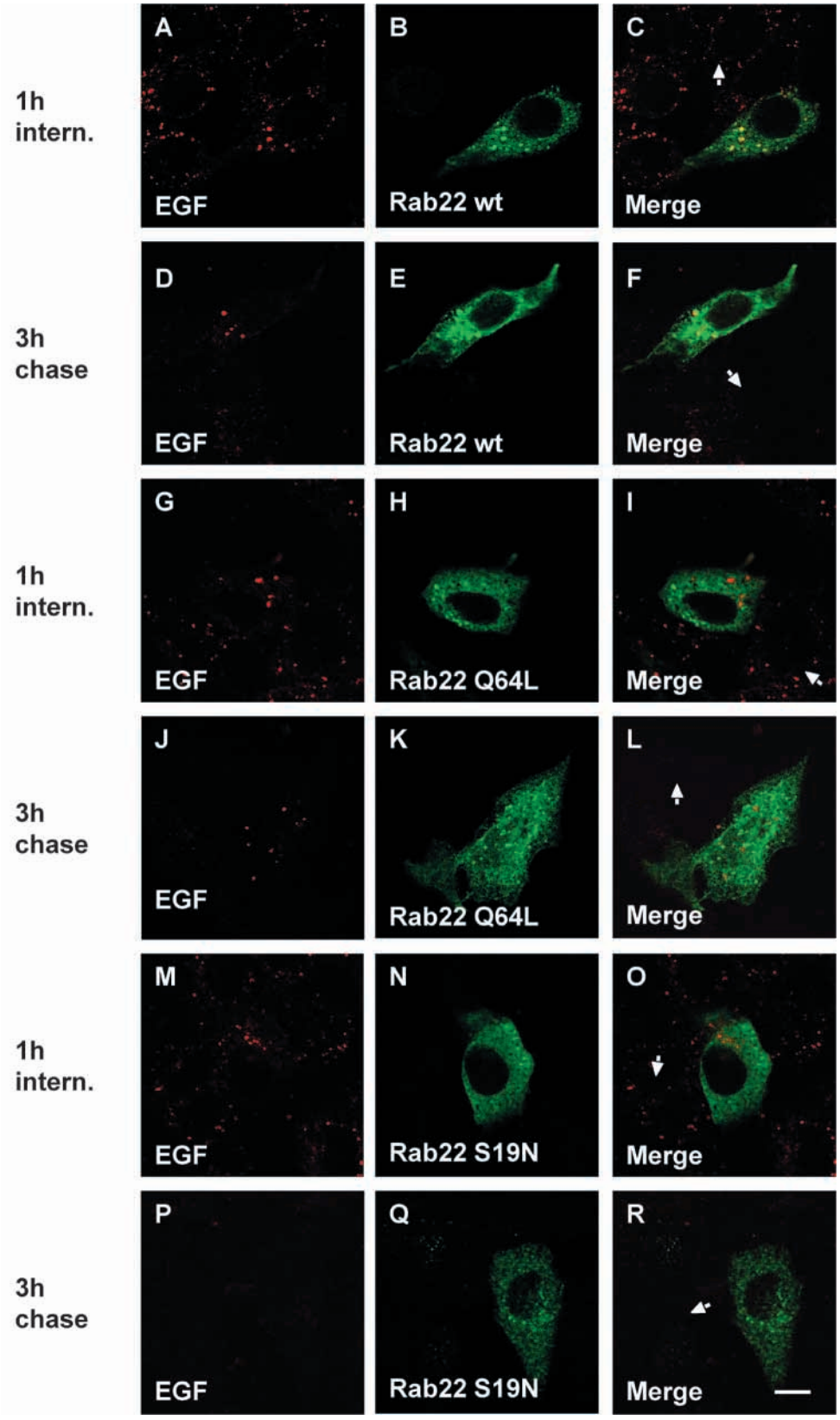

Fig. 5. Effects of Rab22a on the uptake and degradation of rhodamine-conjugated epidermal growth factor (rho-EGF). Hep2 cells were infected with the Ankara strain Vaccinia T7 virus, followed by transfection of myc-tagged Rab22a wt, Q64L or S19N constructs in pGEM-1. Internalization (1 hour) and chase (3 hours) of rho-EGF were then carried out as described in Materials and Methods, and the cells were processed for confocal immunofluorescence microscopy. The rho-EGF fluorescence is shown in panels A,D,G,J,M,P, immunostaining for Rab22a in B,E,H,K,N,Q, and overlays in C,F,I,L,O,R. After the 1 hour internalization period, the rho-EGF was found in intracellular endocytic structures, the volume and distribution of which were highly similar in untransfected cells (arrows) and those expressing wt Rab22a (A-C), Rab22 Q64L (G-I) or Rab22 S19N (M-O). After 3 hours chase, the rho-EGF fluorescence had disappeared from untransfected cells and those expressing Rab22 S19N (P-R), although it remained detectable in cells expressing Rab22a wt (D-F) or the Q64L mutant (J-L). Colocalization of Rab22a wt (C,F) but not Q64L (I,L) was detected with the rho-EGF positive structures. Bar=10 μm.

edges (Fig. 4F-H). Expression of the S19N mutant had no obvious effect on the amount or distribution of the internalized Tfn (Fig. 4I-K). The kinetics of transferrin internalization and recycling was studied in COS-1 cells transfected with the Rab22a wt, Q64L or S19N pcDNA3.1 constructs, using biotinylated human Tfn. As compared to untransfected or mock-transfected (with the pcDNA3.1 vector) COS-1 cells, the cells expressing Rab22a wt, S19N, or Q64L showed no significant difference in the kinetics of either biotin-Tfn uptake or recycling (data not shown). These results suggest that Rab22a does not regulate the transferrin cycle. However, the redistribution of Tfn-positive structures to the leading edges of cells that express the Q64L mutant indicates a possible role of Rab22a in regulation of endosome motility.

The impact of Rab22a on membrane trafficking along the endocytic pathway was further investigated by monitoring the uptake and degradation of rhodamine-labeled epidermal growth factor (EGF) in Hep2 cells expressing the wt GTPase or its mutant forms. Hep2 provided a cell system feasible for this analysis owing to their efficient EGF binding and uptake. The rho-EGF was internalized for 1 hour, followed by a 3 hour chase before fixation of the cells

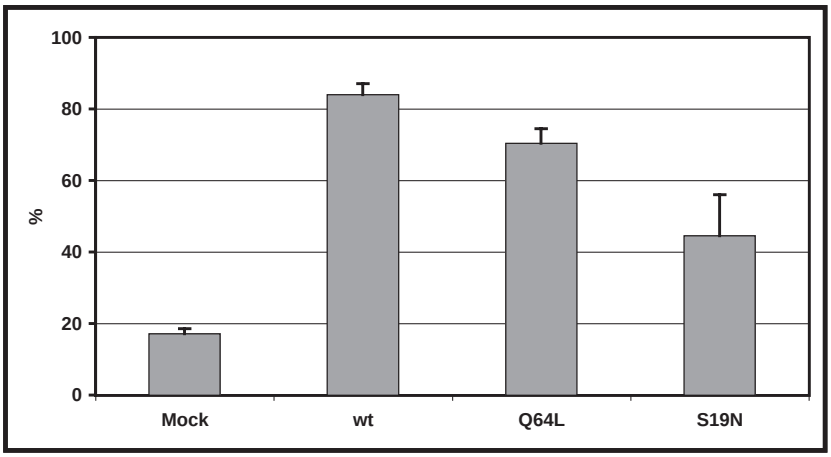

Fig. 6. Quantitation of the effects of Rab22a on rho-EGF degradation in Hep2 cells. Hep2 cells were transfected with pGEM-myc, -mycRab22a wt, -mycRab22a Q64L or -mycRab22a S19N using the Vaccinia system. The cells were incubated with rhodamine-labelled EGF for 1 hour at 37°C, followed by a 3 hour chase at 37°C before fixation and staining with an anti-myc antibody. Transfected cells were visualized by confocal immunofluorescence microscopy, and 150 cells on separate coverslips were counted for the presence of rho-EGF signal after a 3 hour chase. The data are presented as the % (±s.e.m.) of transfected cells having a visible rho-EGF signal after the chase.

and confocal microscopic observation of the labeled marker and the expressed GTPase. After 1 hour, the rho-EGF was found in Rab22a-positive endosomal structures, whose volume and distribution were highly similar in untransfected cells and those expressing wt Rab22a (Fig. 5A-C). However, a significant difference between untransfected and Rab22a expressing cells was apparent after a 3 hour chase: the rho-EGF fluorescence was no longer observed in the untransfected cells due to degradation of the growth factor, whereas it remained detectable in the Rab22a positive cells and colocalized significantly with the expressed GTPase (Fig. 5D-F). The same effect, albeit less pronounced, was observed in cells expressing Rab22a Q64L (Fig. 5G-L). Interestingly, although both Rab22a wt and Q64L clearly inhibited the degradation of the rho-EGF, the Q64L mutant did not colocalize with the marker after the 1 hour internalization period or after the 3 hour chase. Degradation of rho-EGF proceeded in a normal fashion in a majority of the cells expressing the S19N mutant (Fig. 5M-R).

The effects of Rab22a and the two mutants on rho-EGF degradation were quantified by calculating the proportion of the transfected cells that displayed rho-EGF positive endosomal elements after the 3 hour chase (Fig. 6). The highest frequency of such cells was observed in cultures expressing wt Rab22a (84%), the percentage in Q64L expressing ones being somewhat lower (70%). Also in cells expressing the S19N mutant the frequency (44%) was elevated compared to mock-transfected cells (17%), but the statistical variance of the results in the S19N expressing cells was high.

To elucidate the effects of Rab22a on fluid phase endocytosis, internalization and trafficking of TRITC-dextran were monitored in BHK-21 cells expressing wt Rab22a or its mutant forms. The transfected BHK-21 cells were allowed to endocytose TRITC-dextran for 1 hour, followed by a 3 hour chase incubation. The cells were then double immunostained for EEA1 and LAMP-1; in some experiments they were alternatively stained for Rab22a. In mock-transfected cells, dextran that had been internalized for 1 hour was found partly in EEA1-positive early endosomes and partly in LAMP-1-positive later compartments (not shown). During a 3 hour chase, it was chased to late structures, which showed no overlap with EEA1 but coincided to a large extent with LAMP-1 (Fig. 7A-E). In a majority of cells expressing wt Rab22a, the trafficking of TRITC-dextran proceeded as in the mock-transfected ones. Even though EEA1 was redistributed in the large vacuole-like endosomal structures induced by the GTPase, the internalized marker showed no colocalization with the EEA1 after the 3 hour chase but reached the LAMP-1-positive late endosomes/lysosomes (Fig. 7F-J). In cells expressing the Q64L mutant the situation was, however, different. The TRITC-dextran was found in the Rab22a Q64L-induced large vacuolar endosomes, which contained markers of both early (EEA1) and late (LAMP-1) endosomes (Fig. 7K-O), both after the 1 hour internalization and after the 3 hour chase. Mixing of the endosomal markers was most prominent in the largest Q64L-induced vacuolar structures. Expression of the S19N mutant had no apparent effect on transport of the internalized marker to LAMP-1-positive compartments (Fig. 7P-T). Quantification of the internalized TRITC-dextran after the 1 hour uptake period, carried out using the Leica LCS software, revealed no significant changes in fluid-phase uptake induced by Rab22a wt or either of the mutants as compared to untransfected cells (data not shown). These results suggest that the uptake or the trafficking of a fluid phase marker to late endocytic compartments marker is not markedly affected by wt Rab22a. However, the Q64L mutant causes mixing of early and late endosomal elements and creates an abnormal fusion compartment in which the fluid-phase marker accumulates.

To elucidate the possible effects of Rab22a on protein trafficking from the biosynthetic pathway to endosomes/lysosomes, we monitored the effects of the overexpressed wt or mutant proteins on the transport of coexpressed human aspartylglucosaminidase (AGA), a lysosomal hydrolase that is routed to endosomes via the M6PR-mediated pathway (Enomaa et al., 1995; Tikkanen et al., 1997). The proteins were expressed in BHK-21 cells for 24 hours, followed by a 3 hour incubation in the presence of cycloheximide to chase the AGA from the biosynthetic pathway to lysosomes. The cells were then triple immunostained for AGA, EEA1 and LBPA. In some experiments, the LBPA staining was omitted and the expressed Rab22a was visualized using anti-myc mAb. In mock-transfected cells the AGA was chased to EEA1-negative vesicles/sites that contained the late endocytic pathway marker LBPA (Fig. 8A-E). As in the case of TRITC-dextran, the transport of AGA into late endosomes/lysosomes proceeded in a normal fashion in a majority of cells overexpressing wt Rab22a and displaying the enlarged EEA1-

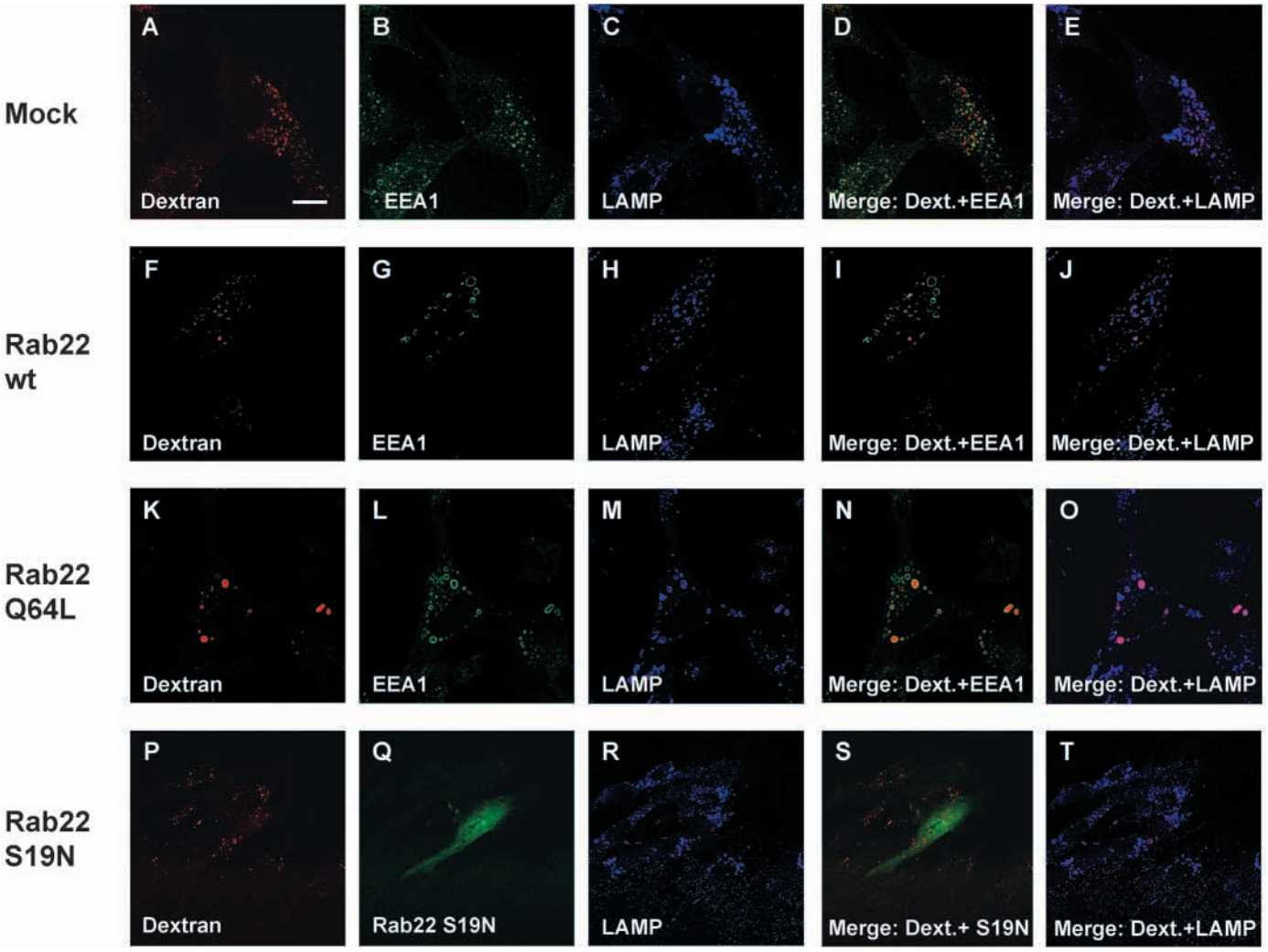

Fig. 7. The effect of Rab22a on the endocytic trafficking of internalized TRITC-dextran. BHK-21 cells were transfected (for 24 hours) with the mycRab22a wt, Q64L or S19N cDNAs (indicated on the left) in pcDNA3.1 or the plain vector plasmid (Mock), followed by 1 hour internalization of TRITC-dextran and a 3 hour chase in the absence of the compound. The cells were then immunostained for EEA1 and LAMP-1 and viewed under a confocal microscope. TRITC-dextran fluorescence is shown in panels A,F,K,P, staining for EEA1 in B,G,L, LAMP-1 staining in C,H,M,R, and Rab22a staining in Q. Pairwise overlays of the channels are shown in D,E,I,J,N,O,S and T. In mock-transfected cells the TRITC-dextran was transported to structures that contained LAMP-1 and showed no overlap with the early endosome marker EEA1 during the chase (A-E). In cells expressing Rab22a wt, the transport of TRITC-dextran proceeded in a similar fashion, despite the presence of abnormally large EEA1-positive vacuolar endosomes induced by the GTPase (F-J). In a majority of cells expressing Rab22a Q64L, however, the fluorescent dextran ended up in large vacuolar endosomes which now contained markers of both early (EEA1) and late (LAMP-1) endocytic compartments (K-O). Expression of the S19N mutant had no detectable effect on the trafficking of TRITC-dextran (P-T). In Q, staining for the Rab is shown instead of EEA1, as S19N-expressing cells cannot be identified on the basis of their endosome morphology. Bar=10 μm.

positive early endosomes (Fig. 8F-J). In most (>85%) of the cells expressing Rab22a Q64L, however, the AGA accumulated in abnormal vacuolar endocytic compartments, which were positive for both EEA1 and LBPA (Fig. 8K-O). Accumulation of AGA in the large spherical endosomes was not inhibited by 5 mM mannose-6-phosphate included in the growth medium (data not shown), suggesting that AGA was transported into these structures mainly from the TGN rather than via the cell surface. Expression of Rab22a S19N had no apparent effect on the trafficking of AGA (Fig. 8P-T). Intriguingly, Rab22a Q64L was not detected on all large vacuolar endosomes that contained accumulated AGA or TRITC-dextran (not shown).

Effects of Rab22a overexpression on the Golgi apparatus

Prompted by the observed abnormal trafficking of AGA, a marker originating from the biosynthetic pathway, in cells transfected with the Rab22a Q64L construct, we carried out triple staining of Rab22 wt or mutant-expressing BHK-21 and HeLa cells for the expressed GTPase, for markers of the Golgi apparatus (antibodies against GM-130 or mannosidase II) and for EEA1. While Rab22a S19N was without effect on Golgi morphology, high-level expression of wild type or Q64L Rab22a in HeLa cells caused a complete vesiculation of the Golgi apparatus (Fig. 9). The expressed wt and Q64L Rab22a were found to colocalize significantly with the GM130-positive Golgi fragments. The dispersed Golgi elements did not contain

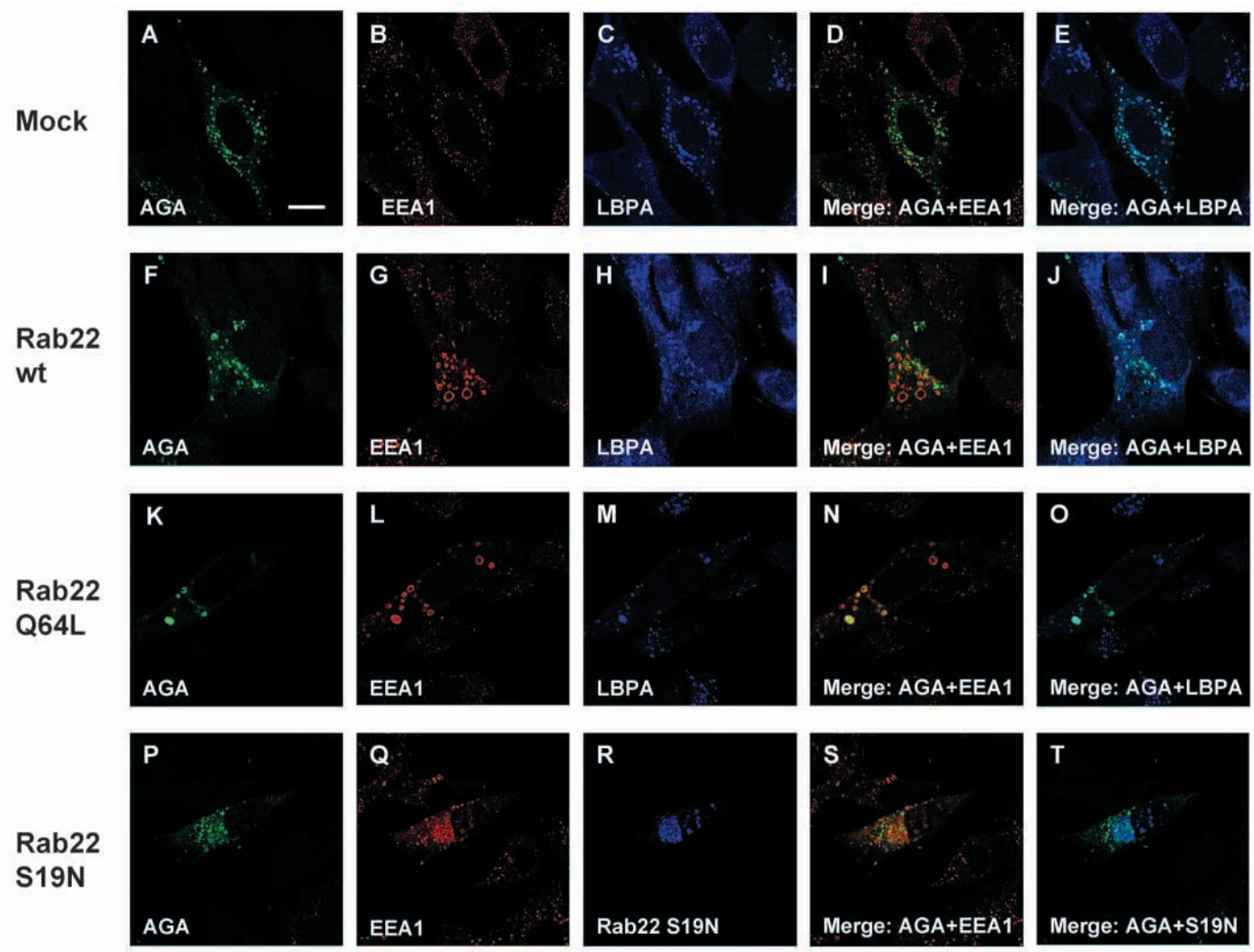

Fig. 8. The effect of Rab22a on the transport of aspartylglucosaminidase (AGA) to lysosomes. BHK-21 cells were double transfected for 24 hours with Rab22a wt or mutant cDNAs (indicated on the left) in pcDNA3.1 or the plain vector plasmid (Mock) and human AGA cDNA in pSVPoly, followed by a 3 hour chase in the presence of cycloheximide (25 μg/ml). Thereafter the cells were triple immunostained for AGA, EEA1 and LBPA, and viewed under a confocal microscope. Staining for AGA is shown in panels A,F,K,P, for EEA1 in B,G,L,Q, and for LBPA in C,H,M,R. Pairwise overlays of the channels are shown in D,E,I,J,N,O,S and T. In mock-transfected cells (A-E), the AGA was chased into punctate structures that colocalized with the late endosome/lysosome marker LBPA but not with EEA1. In a majority of cells expressing the wt Rab22a, the trafficking of AGA to late endocytic compartments proceeded in a similar fashion, despite the presence of enlarged EEA1-positive endosomes induced by the GTPase (F-J). In cells expressing the Q64L mutant, however, AGA accumulated in large vacuolar endosomes, which contained both early (EEA1) and late (LBPA) endosomal markers (K-O). Expression of the Rab22a S19N mutant had no significant effect on the transport of AGA to late endocytic compartments (P-T). Bar=10 μm.

EEA1, indicating that no significant mixing had occurred between the Golgi and endosomes. Fragmentation of the Golgi was also detected in BHK cells expressing wt Rab22a or the Q64L mutant, but the effect was evident here only in occasional cells (data not shown). The effect on Golgi morphology was specific for Rab22, as it was not observed upon overexpression of wild-type or GTPase-deficient mutants of Rab4, Rab5, Rab7 or Rab11 (not shown). These results are consistent with the idea that Rab22a may regulate the trafficking between the Golgi and early endosomes.

Discussion

In the present study we have analyzed the intracellular localization and function of Rab22a. We show that wild-type Rab22a localizes in BHK cells to EEA1-positive early endosomal structures, which increase in size upon overexpression of the small GTPase, as well as on the plasma membrane. It is noteworthy that in BHK cells expressing wt Rab22a the normal small EEA1-positive early endosomes were practically absent and most of the EEA1 appeared to be collected in the large vacuole-like endosomes. Therefore, Rab22a seems to be able to cause fusion of early endosomes to enlarged structures, reminiscent of the phenomenon caused by overexpression of the GTPase-deficient Q79L mutant of Rab5a (Stenmark et al., 1994; Barbieri et al., 1996). In fact, when wt Rab22a and Rab5 Q79L are coexpressed in the same cells, the proteins colocalize in the large vacuolar endosomes (not shown).

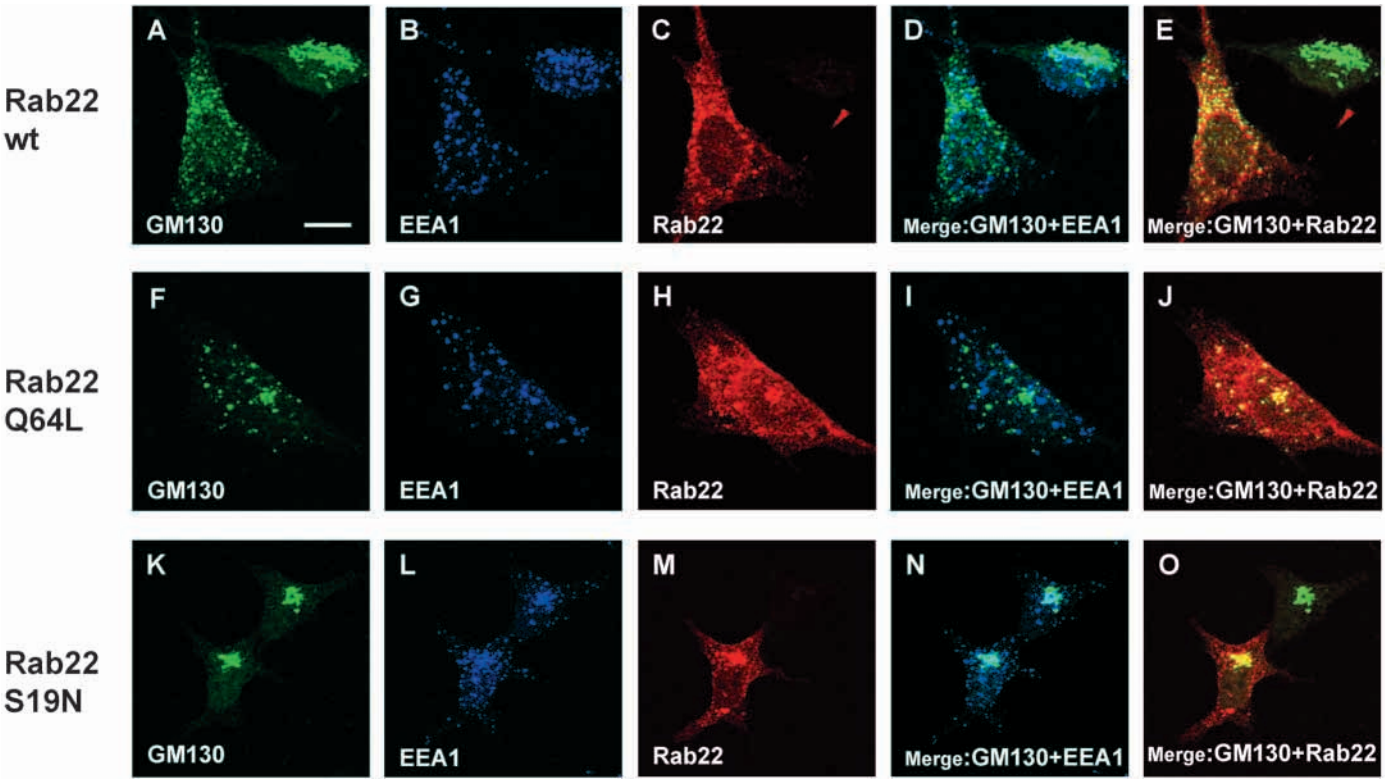

Fig. 9. The effect of Rab22a expression on Golgi apparatus morphology in HeLa cells. Rab22a or its mutant forms were expressed with the Vaccinia T7 system, and the cells were processed for immunofluorescence microscopy; triple stainings with antibodies against GM130, EEA1 and the expressed Rab were carried out. A-E: cells expressing wt Rab22a; F-J: cells expressing the Q64L mutant; K-O, cells expressing the S19N mutant. A,F,K, GM130 staining; B,G,L, EEA1 staining; C,H,M, Rab22a staining. Overlays are shown in D,E,I,J,N and O. The wt Rab22a and the Q64L mutant cause a complete fragmentation of the Golgi apparatus and colocalize significantly with both GM130 and EEA1. No significant mixing of the Golgi and early endosome markers is detected. An untransfected cell with a compact Golgi is seen, for example, in the upper right-hand corner of panel A. The S19N mutant shows colocalization with GM130 but does not induce any redistribution of the Golgi apparatus. Bar=10 μm.

Since overexpression of wt Rab5a does not readily cause such drastic morphological effects, it seems that Rab22a is a more potent stimulator of early endosome fusion than Rab5a.

Interestingly, we found that, like Rab5, GTP-bound Rab22a specifically interacts with the early endosomal FYVE-finger protein EEA1. However, although Rab5 binds to both the N-terminal and the C-terminal regions of EEA1 (Simonsen et al., 1998a), Rab22a only interacts with the EEA1 N-terminus. Furthermore, on the basis of the results of our in vitro binding assay it seems that Rab22a shows higher affinity for the EEA1 N-terminal region than Rab5 does. The finding that Rab22a only binds to one end of EEA1 implies that its function is essentially distinct from that of Rab5. The Rab5-EEA1 interaction has been shown to play a central role in homotypic and heterotypic fusion in the early endocytic pathway (Christoforidis et al., 1999), a process in which Rab5 resides on both apposed membranes and EEA1 can be linked to Rab5 at its both ends, leading to formation of symmetrical bridges of Rab5 and the bound effector. The Rab22a-EEA1 interaction alone cannot lead to the generation of such symmetrical bridges. Instead, Rab22a could participate in membrane interactions in which the other end (C-terminus) of EEA1 is bound to PtdIns-3-P and Rab5. Accordingly, Rab22 should, in principle, have the capacity to control fusion of early endosomes, as suggested by our morphological data. However, if active Rab22a is also localized on transport vesicles originating, for example, from the trans-Golgi network, the interaction with the N-terminus of EEA1 may provide a mechanism through which these vesicles could be tethered at their early endosomal targets.

In studies employing Alexa- or biotin-conjugated transferrin to monitor the receptor-mediated uptake or recycling of this protein, transient overexpression of wt Rab22a or the Q64L or S19N mutants had no significant effect. Therefore, it seems that the function of early endosomal compartments in receiving cargo from the cell surface or recycling molecules is not severely disturbed by overexpression of the GTPase. Further, the lack of detectable effects on transferrin recycling is in accordance with the observed lack of colocalization between Rab22a and the recycling endosome marker Rab11. However, overexpression of the GTPase-deficient Rab22a Q64L did have a marked effect on the intracellular distribution of Alexa-Tfn: instead of being dispersed in the cytoplasm as in non-transfected cells, the Alexa-Tfn-containing endosomal elements were found clustered at the leading edges of the cells. This indicates that Rab22a may, like its closest homologue Rab5 (Nielsen et al., 1999), play a role in regulating the motility and intracellular distribution of early endosomal elements. Intriguingly, the expressed Rab22a Q64L did not colocalize with the peripherally localized Alexa-Tfn-positive elements. This could be due to 1) the ability of the GTPase-deficient mutant to cause a change in the motility of the

Tfn-containing endosomes through a very transient interaction with these elements or, more likely, to the 2) sequestration by Rab22a Q64L of a cytosolic factor that is required for the normal localization of the Tfn-containing endosomes.

As in the experiments measuring Tfn uptake, no obvious effect of wt or mutant Rab22a was observed on the internalization of rhodamine-EGF from the surface of Hep2 cells. However, especially the wt Rab22a but also the Q64L mutant were found to inhibit rho-EGF degradation. It has been reported that EGF-EGF receptor complexes are routed to lysosomal degradative compartments through distinct maturing multivesicular body (MVB)-type, LAMP- and M6PR-negative, structures (Futter et al., 1996). The results thus suggest that wt Rab22a and the activated Q64L mutant interfere with the formation of such MVBs or their ability to interact with lysosomes. Alternatively, changes in the endocytic pathway organization induced by Rab22a (see below) may have disturbed the degradative function of lysosomes.

In BHK-cells, the Q64L mutant disturbed the transport of AGA, a lysosomal hydrolase routed to endosomes via the M6PR pathway, and an internalized fluid-phase marker, TRITC-dextran, which accumulated in large vacuole-appearing structures. These structures contained markers of both early and late endosomes. Formation of such abnormal fusion compartments is not unique to Rab22a: it has also been detected in cells expressing the GTPase-deficient Q79L mutant of Rab5a (d'Arrigo et al., 1997) or an ATPase-deficient mutant of mouse SKD1, a homologue of *S. cerevisiae* Vps4p (Yoshimori et al., 2000). The data indicate that upon increasing overexpression of Rab22a Q64L, the enlarged early endosomes appear first and then also start to acquire late endosomal markers. It is thus possible that the process is due to enhanced retrograde transport from late to early compartments. If one, on the other hand, considers the models of endosomal maturation and the possibility that maturing early endosome subdomains could acquire late endosomal constituents by kiss-and-run type interactions (Storrie and Desjardins, 1996), the Rab22a Q64L mutant phenotype could arise from abnormally enhanced kiss-and-run contacts.

Strikingly, the wt protein and the Q64L mutant also caused, in HeLa cells, a complete vacuolization of the Golgi apparatus and a similar but less prominent effect in BHK cells. This unique finding, together with the partial colocalization of Rab22a with a Golgi marker in HeLa cells, suggests that Rab22a may have a function in the communication between Golgi and early endosomes (see Press et al., 1998; Juuti-Uusitalo et al., 2000; Johannes and Goud, 2000; Sandvig and van Deurs, 2000). The finding that EEA1, a binding partner of Rab22a, also binds syntaxin 6 (Simonsen et al., 1999), provides a possible mechanistic link between Rab22 function and TGN to endosome trafficking. Syntaxin 6 localizes mainly to the trans-Golgi network (Bock et al., 1997) and is implicated in several transport events involving the TGN (Wendler and Tooze, 2001). It is interesting to note that a possible yeast homologue of EEA1, Vac1p, regulates TGN to endosome trafficking (Peterson et al., 1999; Tall et al., 1999). Thus, Rab22a-induced recruitment of EEA1 as a tethering factor in heterotypic contacts between TGN-derived and early endosome membranes could possibly facilitate the local assembly of a syntaxin 6-containing SNARE complexes. Further, it will be interesting to elucidate if Rab22a also binds rabenosyn-5 (Nielsen et al., 2000), a novel effector of Rab5 and a functional homologue of yeast Vac1p. In order to resolve the directionality of the trafficking step(s) regulated by Rab22a, it will be informative to study the role of this protein in the intoxication by Shiga toxin, which is believed to enter the TGN via early endosomes (Johannes and Goud, 2000; Sandvig and van Deurs, 2000).

The question of why Rab22a causes a fragmentation of the Golgi apparatus is intriguing. On the basis of studies of Rab1, it has been suggested that the same Rab could bind tethering factors at both the donor and the acceptor compartments in a vesicular transport step (Moyer et al., 2001). Thus, Rab22a might interact with an unidentified Golgi tethering protein, in addition to with EEA1 (see Barr, 1999), and when present in excess amounts, it disturbs the function of this factor, resulting in organelle fragmentation. On the other hand, the observed effect on endosome motility indicates that Rab22a may interfere with the function of microtubule motor proteins or proteins tethering membrane organelles to microtubules, which could also lead to redistribution of the Golgi apparatus.

We are grateful to Seija Puomilahti, Pirjo Ranta and Eva Rønning for expert technical assistance. Johan Peränen is thanked for kindly providing the pGAT-4 expression vector, Anu Jalanko for the AGA expression construct and anti-human AGA antiserum, Jean Gruenberg for the anti-LAMP-1 and anti-LBPA antibodies, and Ban-Hock Toh for the human EEA1 autoantiserum. The study was supported by the EU TMR programme (ERBFMRXCT960020), the Academy of Finland (grants 42163, 45817, and 50641 to V.M.O.), the Sigrid Juselius Foundation (V.M.O.), the Novo-Nordisk Foundation (H.S.) and the Research Council of Norway (H.S.). M.K. is a member of the Helsinki Graduate School of Biotechnology and Molecular Biology. A.S. is a postdoctoral fellow of the Norwegian Cancer Society.

References

Barbieri, M. A., Li, G., Mayorga, L. S. and Stahl, P. D. (1996). Characterization of Rab5:Q79L-stimulated endosome fusion. *Arch. Biochem. Biophys.* **326**, 64-72.

Barr, F. A. (1999). A novel Rab6-interacting domain defines a family of Golgi-targeted coiled-coil proteins. *Curr. Biol.* **9**, 381-384.

Bock, J. B., Klumperman, J., Davanger, S. and Scheller, R. H. (1997). Syntaxin 6 functions in trans-Golgi network vesicle trafficking. *Mol. Biol. Cell* **8**, 1261-1271.

Bucci, C., Parton, R. G., Mather, I. H., Stunnenberg, H., Simons, K., Hoflack, B. and Zerial, M. (1992). The small GTPase Rab5 functions as a regulatory factor in the early endocytic pathway. *Cell* **70**, 715-728.

Bucci, C., Thomsen, P., Nicoziani, P., McCarthy, J. and van Deurs, B. (2000). Rab7: a key to lysosome biogenesis. *Mol. Biol. Cell* **11**, 467-480.

Chavrier, P. and Goud, B. (1999). The role of ARF and Rab GTPases in membrane transport. *Curr. Opin. Cell Biol.* **11**, 466-475.

Chen, D., Guo, J., Miki, T., Tachibana, M. and Gahl, W. A. (1996). Molecular cloning of two novel rab genes from human melanocytes. *Gene* **174**, 129-134.

Christoforidis, S., McBride, H. M., Burgoyne, R. D. and Zerial, M. (1999). The Rab5 effector EEA1 is a core component of endosome docking. *Nature* **397**, 621-625.

Corvera, S., D'Arrigo, A. and Stenmark, H. (1999). Phosphoinositides in membrane traffic. *Curr. Opin. Cell Biol.* **11**, 460-465.

D'Arrigo, A., Bucci, C., Toh, B. H. and Stenmark, H. (1997). Microtubules are involved in bafilomycin A1-induced tubulation and Rab5-dependent vacuolation of early endosomes. *Eur. J. Cell Biol.* **72**, 95-103.

Echard, A., Jollivet, F., Martinez, O., Lacapere, J. J., Rousselet, A., Janoueix-Lerosey, I. and Goud, B. (1998). Interaction of a Golgi-associated kinesin-like protein with Rab6. *Science* **279**, 580-585.

Enomaa, N., Danos, O., Peltonen, L. and Jalanko, A. (1995). Correction of deficient enzyme activity in a lysosomal storage disease, aspartylglucosaminuria, by enzyme replacement and retroviral gene transfer. *Hum. Gene Ther.* **6**, 723-31.

Feng, Y., Press, B. and Wandinger-Ness, A. (1995). Rab 7: an important regulator of late endocytic membrane traffic. *J. Cell Biol.* **131**, 1435-1452.
Futter, C. E., Pearse, A., Hewlett, L. J. and Hopkins, C. R. (1996). Multivesicular endosomes containing internalized EGF-EGF receptor complexes mature and then fuse directly with lysosomes. *J. Cell Biol.* **132**, 1011-1023.
Gaullier, J.-M., Simonsen, A., D'Arrigo, A., Bremnes, B., Aasland, R. and Stenmark, H. (1998). FYVE fingers bind PtdIns(3)P. *Nature* **394**, 432-433.
Gruenberg, J. and Maxfield, F. R. (1995). Membrane transport in the endocytic pathway. *Curr. Opin. Cell Biol.* **7**, 552-563.
Guarente, L. (1983). Yeast promoters and lacZ fusions designed to study expression of cloned genes in yeast. *Methods Enzymol.* **101**, 181-191.
Guo, W., Sacher, M., Barrowman, J., Ferro-Novick, S. and Novick, P. (2000). Protein complexes in transport vesicle targeting. *Trends Cell Biol.* **10**, 251-255.
Hoffenberg, S., Sanford, J. C., Liu, S., Daniel, D. S., Tuvin, M., Knoll, B. J., Wessling-Resnick, M. and Dickey, B. F. (1995). Biochemical and functional characterization of a recombinant GTPase, Rab5, and two of its mutants. *J. Biol. Chem.* **270**, 5048-5056.
Hopkins, C. R. (1983). Intracellular routing of transferrin and tranferrin receptors in epidermoid carcinoma A431 cells. *Cell* **35**, 321-330.
Huijbregts, R. P. H., Topalof, L. and Bankaitis, V. A. (2000). Lipid metabolism and regulation of membrane trafficking. *Traffic* **1**, 195-202.
Johannes, L. and Goud, B. (2000). Facing inwards from compartment shores: How many pathways were we looking for? *Traffic* **1**, 119-123.
Juuti-Uusitalo, K., Airanne, K. J., Laukkanen, A., Punnonen, E-L., Olkkonen, V. M., Grüenberg, J., Kulomaa, M. and Marjomäki, V. (2000). Selective targeting of avidin/mannose 6-phosphate receptor chimeras to early or late endosomes. *Eur. J. Cell Biol.* **79**, 458-468.
Kobayashi, T., Stang, E., Fang, K. S., de Moerloose, P., Parton, R. G. and Gruenberg, J. (1998). A lipid associated with the antiphospholipid syndrome regulates endosome structure and function. *Nature* **392**, 193-197.
Liljeström, P. and Garoff, H. (1991). A new generation of animal cell expression vectors based on the Semliki Forest virus replicon. *Bio/technology* **9**, 1356-1361.
Lombardi, D., Soldati, T., Riederer, M. A., Goda, Y., Zerial, M. and Pfeffer, S. R. (1993). Rab9 functions in transport between late endosomes and the trans Golgi network. *EMBO J.* **12**, 677-682.
McBride, H. M., Rybin, V., Murphy, C., Giner, A., Teasdale, R. and Zerial, M. (1999). Oligomeric complexes link Rab5 effectors with NSF and drive membrane fusion via interactions between EEA1 and syntaxin 13. *Cell* **98**, 377-386.
McLauchlan, H., Newell, J., Morrice, N., Osborne, A., West, M. and Smythe, E. (1998). A novel role for Rab5-GDI in ligand sequestration into clathrin-coated pits. *Curr. Biol.* **8**, 34-45.
Mellman, I. (1996). Endocytosis and molecular sorting. *Annu. Rev. Cell Dev. Biol.* **12**, 575-625.
Meresse, S., Gorvel, J. P. and Chavrier, P. (1995). The rab7 GTPase resides on a vesicular compartment connected to lysosomes. *J. Cell Sci.* **108**, 3349-3358.
Moyer, B. D., Allan, B. B. and Balch, W. E. (2001). Rab1 interaction with a GM130 effector complex regulates COPII vesicle cis-Golgi tethering. *Traffic* **2**, 268-276.
Mukhopadhyay, A., Funato, K. and Stahl, P. D. (1997). Rab7 regulates transport from early to late endocytic compartments in *Xenopus* oocytes. *J. Biol. Chem.* **272**, 13055-13059.
Nielsen, E., Severin, F., Backer, J. M., Hyman, A. A. and Zerial, M. (1999). Rab5 regulates motility of early endosomes on microtubules. *Nat. Cell Biol.* **1**, 376-382.
Nielsen, E., Christoforidis, S., Uttenweiler-Joseph, S., Miaczynska, M., Dewitte, F., Wilm, M., Hoflack, B. and Zerial, M. (2000). Rabenosyn-5, a novel Rab5 effector, is complexed with hVPS45 and recruited to endosomes through a FYVE finger domain. *J. Cell Biol.* **151**, 601-612.
Novick, P. and Zerial, M. (1997). The diversity of Rab proteins in vesicle transport. *Curr. Opin. Cell Biol.* **9**, 496-504.
Olkkonen, V. M., Dupree, P., Killisch, I., Lutcke, A., Zerial, M. and Simons, K. (1993). Molecular cloning and subcellular localization of three GTP-binding proteins of the rab subfamily. *J. Cell Sci.* **106**, 1249-1261.
Olkkonen, V. M., Dupree, P., Simons, K., Liljestrom, P. and Garoff, H. (1994). Expression of exogenous proteins in mammalian cells with the Semliki Forest virus vector. *Methods Cell Biol.* **43**, 43-53.
Olkkonen, V. M. and Stenmark, H. (1997). Role of Rab GTPases in membrane traffic. *Int. Rev. Cytol.* **176**, 1-85.
Peterson, M. R., Burd, C. G. and Emr, S. D. (1999). Vac1p coordinates Rab and phosphatidylinositol 3-kinase signaling in Vps45p-dependent vesicle docking/fusion at the endosome. *Curr. Biol.* **9**, 159-162.
Press, B., Feng, Y., Hoflack, B. and Wandinger-Ness, A. (1998). Mutant Rab7 causes the accumulation of cathepsin D and cation-independent mannose 6-phosphate receptor in an early endocytic compartment. *J. Cell Biol.* **140**, 1075-1089.
Ren, M., Zeng, J., De Lemos-Chiarandini, C., Rosenfeld, M., Adesnik, M. and Sabatini, D. D. (1996). In its active form, the GTP-binding protein rab8 interacts with a stress-activated protein kinase. *Proc. Natl. Acad. Sci. USA.* **93**, 5151-5155.
Ren, M., Xu, G., Zeng, J., De Lemos-Chiarandini, C., Adesnik, M. and Sabatini, D. D. (1998). Hydrolysis of GTP on rab11 is required for the direct delivery of transferrin from the pericentriolar recycling compartment to the cell surface but not from sorting endosomes. *Proc. Natl. Acad. Sci. USA* **95**, 6187-6192.
Rodman, J. S. and Wandinger-Ness, A. (2000). Rab GTPases coordinate endocytosis. *J. Cell Sci.* **113**, 183-192.
Sandvig, K. and van Deurs, B. (2000). Entry of ricin and Shiga toxin into cells: molecular mechanisms and medical perspectives. *EMBO J.* **19**, 5943-5950.
Simonsen, A., Lippe, R., Christoforidis, S., Gaullier, J. M., Brech, A., Callaghan, J., Toh, B. H., Murphy, C., Zerial, M. and Stenmark, H. (1998a). EEA1 links PI(3)K function to Rab5 regulation of endosome fusion. *Nature* **394**, 494-498.
Simonsen, A., Bremnes, B., Rønning, E., Aasland, R. and Stenmark, H. (1998b). Syntaxin-16, a putative Golgi t-SNARE. *Eur. J. Cell Biol.* **75**, 223-231.
Simonsen, A., Gaullier, J. M., D'Arrigo, A. and Stenmark, H. (1999). The Rab5 effector EEA1 interacts directly with syntaxin-6. *J. Biol. Chem.* **274**, 28857-28860.
Sönnichsen, B., De Renzis, S., Nielsen, E., Rietdorf, J. and Zerial, M. (2000). Distinct membrane domains on endosomes in the recycling pathway visualized by multicolor imaging of Rab4, Rab5, and Rab11. *J. Cell Biol.* **149**, 901-914.
Stenmark, H., Parton, R. G., Steele-Mortimer, O., Lutcke, A., Gruenberg, J. and Zerial, M. (1994). Inhibition of rab5 GTPase activity stimulates membrane fusion in endocytosis. *EMBO J.* **13**, 1287-1296.
Storrie, B. and Desjardins, M. (1996). The biogenesis of lysosomes: is it a kiss and run, continuous fusion and fission process? *BioEssays* **18**, 895-903.
Sutter, G., Ohlmann, M. and Erfle, V. (1995). Non-replicating vaccinia vector efficiently expresses bacteriophage T7 RNA polymerase. *FEBS Lett.* **371**, 9-12.
Tall, G. G., Hama, H., DeWald, D. B. and Horazdovsky, B. F. (1999). The phosphatidylinositol 3-phosphate binding protein Vac1p interacts with a Rab GTPase and a Sec1 homologue to facilitate vesicle-mediated vacuolar protein sorting. *Mol. Biol. Cell* **10**, 1873-1889.
Tikkanen, R., Peltola, M., Oinonen, C., Rouvinen, J. and Peltonen, L. (1997). Several cooperating binding sites mediate the interaction of a lysosomal enzyme with the phosphotransferase. *EMBO J.* **16**, 6684-6693.
Tisdale, E. J. (2000). Rab2 requires PKCι/λ to recruit B-COP for vesicle formation. *Traffic* **1**, 702-712.
Ullrich, O., Reinsch, S., Urbe, S., Zerial, M. and Parton, R. G. (1996). Rab11 regulates recycling through the pericentriolar recycling endosome. *J. Cell Biol.* **135**, 913-924.
van der Sluijs, P., Hull, M., Webster, P., Male, P., Goud, B. and Mellman, I. (1992). The small GTP-binding protein rab4 controls an early sorting event on the endocytic pathway. *Cell* **70**, 729-740.
van Deurs, B., Holm, P. K., Kayser, L., Sandvig, K. and Hansen, S. H. (1993). Multivesicular bodies in HEp-2 cells are maturing endosomes. *Eur. J. Cell Biol.* **61**, 208-224.
van Deurs, B., Holm, P. K., Kayser, L. and Sandvig, K. (1995). Delivery to lysosomes in the human carcinoma cell line HEp-2 involves an actin filament-facilitated fusion between mature endosomes and preexisting lysosomes. *Eur. J. Cell Biol.* **66**, 309-323.
Waters, M. G. and Hughson, F. M. (2000). Membrane tethering and fusion in the secretory and endocytic pathways. *Traffic* **1**, 588-597.
Wendler, F. and Tooze, S. (2001). Syntaxin 6: The promiscuous behaviour of a SNARE protein. *Traffic* **2**, 606-611.
Vojtek, A. B., Hollenberg, S. M. and Cooper, J. A. (1993). Mammalian Ras interacts directly with the serine/threonine kinase Raf. *Cell* **74**, 205-214.
Yamashiro, D. J., Tycko, B., Fluss, S. R. and Maxfield, F. R. (1984). Segregation of transferrin to a mildly acidic (pH 6.5) para-Golgi compartment in the recycling pathway. *Cell* **37**, 789-800.
Yoshimori, T., Yamagata, F., Yamamoto, A., Mizushima, N., Kabeya, Y., Nara, A., Miwako, I., Ohashi, M., Ohsumi, M. and Ohsumi, Y. (2000). The mouse SKD1, a homologue of yeast Vps4p, is required for normal endosomal trafficking and morphology in mammalian cells. *Mol. Biol. Cell* **11**, 747-763.
Zerial, M. and McBride, H. (2001). Rab proteins as membrane organizers. *Nat. Rev. Mol. Cell. Biol.* **2**, 107-117.